PCCP

Accepted Manuscript

ROYAL SOCIETY OF CHEMISTRY

www.rsc.org/pccp

Nonideal effects in electroacoustics of solutions of charged particles: combined experimental and theoretical analysis from simple electrolytes to small nanoparticles

R. Pusset[a,b*], S. Gourdin-Bertin[a,b], E. Dubois[a,b,*], J. Chevalet[a,b], G. Mériguet[a,b], O. Bernard[a,b], V. Dahirel[a,b], M. Jardat[a,b], D. Jacob[c]

Received Xth XXXXXXXXXX 2015, Accepted Xth XXXXXXXXX 2015
First published on the web Xth XXXXXXXXXX 2015
DOI: 10.1039/b000000x

The electric signal induced by an ultrasonic wave on aqueous solutions of charged species is measured and analyzed. A device is developed which measures the raw induced electric signal for small sample volumes (few milliliters) and without any preceding calibration. The potential difference generated between two identical electrodes, called the ionic vibration potential (IVP), is thus easily deduced. In parallel, a theory for the IVP is built based on a robust analytical theory already used successfully to account for other transport coefficients in electrolyte solutions. From the analysis of the IVP measured for several aqueous electrolyte solutions, which are well defined model systems for this technique, we explain and validate the different contributions to the signal. In particular, the non ideal effects at high concentrations are thoroughly understood. A first step towards colloidal systems is presented with the analysis of the signal in solutions of a polyoxometallate salt, opening determinations of reliable electrophoretic mobilities in dispersions of nanoobjects.

1 Introduction

It has become traditional to assess the ability of charged particles to aggregate from the measurement of their electrokinetic potential or zeta-potential ζ, defined as the electrostatic potential at the plane where slip with respect to bulk solution is postulated to occur[1]. This quantity is often deduced from the electrophoretic mobility measured by optical techniques (laser Doppler velocimetry or Single Plane Illumination Microscopy), that are naturally limited for samples which strongly absorb or scatter light in the visible spectrum. The use of an ultrasound wave instead of light is often a very efficient method to circumvent these pitfalls. The response to an applied acoustic field of a solution containing charged solutes was put forward by Debye in 1933[2] in the case of electrolyte solutions. When an ultrasonic wave is applied to a solution of charged species, particles follow more or less the fluid which oscillates back and forth. According to their respective masses, the particles displacements might differ, generating a transient separation. This minute charge separation creates an electric field which can be measured. The potential difference U generated between two identical electrodes (separated by a gap at any odd number of half wavelength of the ultrasonic perturbation) is generally named the ultrasonic vibration potential (UVP) but more usually the ion vibration potential (IVP, U_{IV}) in electrolyte solutions[3] and the colloid vibration potential (CVP, U_{CV}) in colloidal suspensions[1].

Experimentally, the first quantitative series of measurements were performed on electrolytes[4]. However later, only commercial devices devoted to the analysis of colloidal suspensions in terms of electrokinetic potential ζ were developed. In parallel, the theoretical developments were also the subject of a number of articles, which can be split into two categories whether they refer to electrolyte solutions[2,5–9] or to colloidal suspensions[10–13].

If the historical motivations for the determination of ions properties[2,4,14] have diminished, there is a renewed interest in the signal given by electrolytes due to the development of UVP imaging and the need for quantitative values of IVP[15–17]. Moreover, the background signal of the electrolyte in colloidal dispersions has to be accurately determined in samples where the contribution of the larger particles is small[12,18–20]. Also, contrary to colloids, electrolytes are simple and very well defined systems (size and charge are monodisperse), with many reliable data available in literature. This enables the reliable calculation of their electroacoustic signal. Besides, the ability to detect the signal created in electrolytes opens the way for measuring small signals whatever the system, in particular particles with low charge, density close to the solvent, high

*emmanuelle.dubois@upmc.fr
[a] Sorbonne Universités, UPMC Univ Paris 06, UMR 8234, PHENIX, F-75005, Paris France
[b] CNRS, UMR 8234, PHENIX, F-75005, Paris France
[c] Cordouan Technologies, 11 avenue de Canteranne, 33600 Pessac, France

conductivity, or low concentration. This cannot be done with the current commercial devices for two reasons: firstly, such a small signal cannot be measured and, secondly, the result is given as one value of electrophoretic mobility or zeta potential when measurable, which applies only to strongly asymmetric systems with one dominating species. Last, in the long run, the technique would benefit from a bridge between the two coexisting approaches on electrolytes and colloids. Indeed yet these two approaches do not rely on the same concepts neither do they use the same level of description. Typically, the relevant parameter for the theory of electrolytes[21] is the ionic electric charge Q_i while the electrokinetic potential ζ is used for the electrokinetic theory of colloids[1,22,23]. As for the vocabulary, the term ideal in the theory of electrolytes refers to an ion at infinite dilution, i.e. without interactions with other ions or in other terms, to the limit $\kappa a \ll 1$ with a the radius of the charged particle and κ the inverse of the Debye length. In the electrokinetic theory, ideal means that the double layer around the particle is much thinner than its radius, i.e. $\kappa a \gg 1$. The underlying difference is the dissymmetry between species for colloids, treated as objects in a continuum although electrolytes are treated as cations and anions in a solvent.

In the present study, we begin with a combined theoretical and experimental approach on the simple and well defined electrolyte solutions. The aim is to apply the gathered knowledge to colloidal systems in a second step. Due to their already underlined advantages, electrolyte solutions enable the test of the theoretical descriptions. The base is a robust analytical theory already used successfully to account for other transport coefficients in electrolyte solutions. For example, this theory was proved to be reliable to account for the electrical conductivity of simple electrolytes and of micellar solutions[24,25], for the self-diffusion coefficients of ions and for their mutual diffusion[26,27]. However, in the frame of electroacoustic, several hypothesis need investigation. Moreover, the confrontation of models to experiments is necessary and implies the development of an appropriate setup able to measure the IVP of electrolyte solutions. Given our long term goal and in order to avoid the limitations of the current devices, we aim at (i) measurements on small volumes (few milliliters), (ii) obtention of the raw signal, (iii) evaluation of the uncertainty on the signal, (iv) measurements without a preliminary calibration of the device (contrary to existing devices, which necessitate calibration on colloidal systems). This parallel approach combining experiments and theory enables a validation of several hypothesis of the theoretical descriptions and of the setup, with no need for any adjustable parameter in the experiment or in the theory.

Our paper is organized as follows. Firstly, we present our robust analytic theory of the IVP and discuss its hypothesis with regards to previous theoretical treatments (Section 2). Secondly, we present the principle of our new device in the light of previous experimental works on the subject (Section 3). In the last section, we present our experimental and theoretical results for several simple electrolyte solutions. Finally a first step towards colloids is done with solutions of a tungstosilicate salt, a disymetric electrolyte, which is actually also a nano colloidal suspension.

2 Analytical theory of the IVP

2.1 Historical background

A short summary of the different historical steps involved in the evolution of electroacoustic is important to understand our theoretical treatment. When in 1933 P. Debye wrote his article entitled "A method for the determination of the mass of electrolyte ions"[2], his goal was to determine the hydrated mass of ions, based on the assumption that ions are heavier when hydrated. The dependence of the IVP with mass, charge, self-diffusion coefficient and concentration of ions was predicted by Debye in the ideal case. Another important contribution to the motion of charged species is the buoyancy force, which accounts for the pressure applied on the species. It was predicted by Hermans in 1938[6] even for small ions. It is interesting to note that the main consequence of the buoyancy force is that the solvation water layer is actually invisible: if we add the mass of one water molecule to that of an ion but subtract the buoyancy force created by one molecule of water, we find nearly zero, so we cannot use the method to determine the mass of hydrated ions.

In his famous work on electrical conductivity of electrolyte solution, Onsager[28] introduced several corrections to account for the non ideal behavior of electrolyte solutions, namely the hydrodynamic coupling between ions and the so-called electrostatic relaxation. The latter describes the backward force exerted by the ionic atmosphere of an ion when this ion moves forward. Onsager introduced these corrective forces only on the forces applied to ions induced by the electric field. Later, Oka did the same in his paper on the ion vibration potential[5]. However, inertia can also induce a corrective coupling. Actually, Oka's formalism predicts in every case the same behavior of the IVP at high concentration, namely an increase with concentration, but as we proceed to show, this is not the case for every salt. The theory proposed by Oka thus does not significantly improve that of Debye. Later, the buoyancy force introduced by Hermans[6] was not always taken into account for electrolytes. Hovorka, Yeager and Bugosh[7] accounted for it in their paper of 1947, however more recently Durand-Vidal et al.[8,9] in 1995 did not explicitly, due to the lack of definition of pressure gradients for ions with sizes similar to that of a water molecule. On the other hand, an important improvement of the theoretical treatment was proposed by Durand-Vidal et al.[8,9] who applied the hydrodynamic and electrostatic

relaxation corrections to both electrostatic and inertial forces. Moreover, Durand-Vidal used the mean-spherical approximation (MSA) to determine the equilibrium pair correlation functions between ions to estimate these forces. We propose here to develop a theory of the IVP very close to that proposed by Durand-Vidal et al.[8,9] and to take into account the buoyancy force. As we proceed to show in Section 4, experimental results evidence that this contribution to the force must be taken into account even for small ions. Debye combined the Newton's equation of dynamics to the equation of continuity and to the equation of Maxwell-Gauss. We also add here the buoyancy force, as proposed by Hermans[6]. This force takes into account the pressure field and not only the velocity field of the acoustic wave and depends on the volume of solute particles. This quantity is unambiguously defined for colloids. For ions, it can be shown that the appropriate volume is the partial molar volume at fixed temperature and pressure[29]. This demonstration assumes that only water bound to the ion undergoes electrostriction. In the equations, it leads to the substitution of the mass m_i of species i by an effective mass m_i^*, with $m_i^* = m_i - \rho_s V_i / N_A$, where ρ_s is the density of the solvent, V_i the partial molar volume of species i and N_a the Avogadro number. Experimental evidences that the term due to the buoyancy force is necessary will be shown in the section presenting the experimental results.

Newton's equation applied to an ion i with effective mass m_i^* reads:

$$\begin{aligned} m_i^* \frac{\mathrm{d}\boldsymbol{v_i}}{\mathrm{d}t} &= \boldsymbol{F}_i^{\mathrm{el}} + \boldsymbol{F}_i^{\mathrm{friction}} \\ &= Q_i \boldsymbol{E} - \gamma_i (\boldsymbol{v_i} - \boldsymbol{v_s}) \end{aligned} \tag{1}$$

with Q_i the charge of ion i, $\boldsymbol{v_i}$ its velocity, $\boldsymbol{v_s}$ the velocity of the solvent, γ_i its friction constant towards the solvent and $\boldsymbol{E}$ the electric field (induced by acoustic excitation). γ_i is equal to $k_B T / D_i^\circ$, $k_B T$ being the thermal energy and D_i° the diffusion coefficient of i at infinite dilution. The continuity equation, or of mass conservation reads:

$$\frac{\partial C_i}{\partial t} + \boldsymbol{\nabla} \cdot (C_i \boldsymbol{v}_i) = 0 \tag{2}$$

with C_i the number concentration of ion i. The Maxwell-Gauss equation, which links charge densities and electric field $\boldsymbol{E}$, is

$$\boldsymbol{\nabla} \cdot \boldsymbol{E} = \frac{\sum_i C_i Q_i}{\varepsilon_0 \varepsilon_r} \tag{3}$$

with ε_0 the permittivity of the vacuum and ε_r the relative permittivity of the solvent. Then, it is assumed that the acceleration of particle i is equal to that of the solvent of velocity $\boldsymbol{v}_s$, and that the induced electric field is linear as a function of the solvent velocity. Using complex notation, ω being the angular frequency, and expanding to first order, we find:

$$-\mathrm{j}\omega\varepsilon_0\varepsilon_r \boldsymbol{E} = \sum_i C_i Q_i \frac{D_i^\circ}{k_B T} (Q_i \boldsymbol{E} - \mathrm{j}\omega m_i^* \boldsymbol{v}_s) \tag{4}$$

which leads to

$$\boldsymbol{E} = \mathrm{j}\omega \boldsymbol{v}_s \frac{\sum_i \frac{C_i Q_i D_i^\circ}{k_B T} m_i^*}{\mathrm{j}\omega\varepsilon_0\varepsilon_r + \sum_i \frac{C_i Q_i D_i^\circ}{k_B T} Q_i} \tag{5}$$

The IVP is the electric potential difference U_{IV} obtained by integration of equation 5. It can be rewritten in terms of acoustic pressure difference Δp

$$\begin{aligned} U_{IV} &= \frac{-\mathrm{j}\boldsymbol{E}\cdot\boldsymbol{k}}{k^2} \\ &= \frac{\Delta p}{\rho_s} \frac{\sum_i \frac{C_i Q_i D_i^\circ}{k_B T} m_i^*}{\mathrm{j}\omega\varepsilon_0\varepsilon_r + \sum_i \frac{C_i Q_i D_i^\circ}{k_B T} Q_i} \end{aligned} \tag{6}$$

$\boldsymbol{k}$ being the wave-vector of the acoustic wave, ρ_s the density of the solvent. This result may also be written as

$$U_{IV} = \frac{\Delta p}{\rho_s} \frac{\sum_i C_i m_i^* \mu_i^\circ}{K^*(\omega)} \quad = \frac{\Delta p}{\rho_s} \frac{\sum_i C_i m_i^* \mu_i^\circ}{(\mathrm{j}\omega\tau_D + 1) K} \tag{7}$$

with μ_i° being the electric mobility of species i at infinite dilution ($\mu_i^\circ = Q_i D_i^\circ / k_B T$), $K^*(\omega)$ the ideal complex conductivity ($K^*(\omega) = \mathrm{j}\omega\varepsilon_0\varepsilon_r + \sum_i C_i Q_i \mu_i^\circ$), K the real part of the ideal conductivity ($K = \Re(K^*(\omega)) = \sum_i C_i Q_i \mu_i^\circ$) and τ_D the Debye time, i.e. the time of disappearance of charges inhomogeneities in solution. The Debye time τ_D in the present case is exactly the inverse of the so-called Maxwell-Wagner frequency ω_{MW} defined as the conductivity of the medium divided by its permittivity.

These simple formula (6) and (7) allow one to predict easily the behaviour of the ion vibration potential as a function of the ionic concentration: a linear increase at low concentration (the numerator is linear and the denominator is almost constant), and a constant value at high concentration (both numerator and denominator are linear in concentration).

Actually, the low concentration regime corresponds to a Debye time high compared to the period of the acoustic wave ($\omega\tau_D \gg 1$), and the high concentration regime corresponds to a Debye time low compared to the period of the acoustic wave ($\omega\tau_D \ll 1$). At high frequency ($\omega\tau_D \gg 1$), charges do not dissipate on the acoustic time scale, and the electric field is created by the pure charge accumulation, so that the complex conductivity reduces to its imaginary part $\mathrm{i}\omega\varepsilon_0\varepsilon_r$. At low frequency, charges have the time to dissipate, namely the created electric field counteracts the charge accumulation, i.e. the electric current created by the electric field is the opposite of the electric current generated by the acoustic wave. In the low frequency regime, the complex conductivity $K^*(\omega)$ reduces to its real part K. The limit between these asymptotic behaviors corresponds to $\omega\tau_D = 1$, which is of the order of 5×10^{-4} mol L^{-1} for small ions in water at ambient temperature.

Finally, in what follows, we shall investigate only binary electrolyte solutions, which contain only two different ionic species. In addition, to remove the dependence of the signal on the pressure of the acoustic wave p, we introduce the coefficient $S_{\mathrm{IV}} = U_{\mathrm{IV}}/\Delta p$, which reads, thanks to the electroneutrality of the binary electrolyte:

$$S_{\mathrm{IV}} = \frac{U_{\mathrm{IV}}}{\Delta p} = \frac{1}{\rho_{\mathrm{s}}} \frac{1}{\mathrm{j}\omega\tau_{\mathrm{D}} + 1} \frac{D_+^\circ m_+^* - D_-^\circ m_-^*}{D_+^\circ Q_+ - D_-^\circ Q_-} \tag{8}$$

2.2 Calculation of the corrections: analytical theory based on the MSA

In addition to the model described in the previous section, we add the two corrective forces described in section 2.1, namely the hydrodynamic and the electrostatic relaxation forces. The hydrodynamic force $\boldsymbol{F}^{\mathrm{hyd}}$ accounts for the hydrodynamic coupling between solute velocities and is usually referred to as an electrophoretic force. As an ion moves forward, it draws the solvent in the same direction and thus takes also its counterions, which are locally in excess, forward. The electrostatic relaxation force $\boldsymbol{F}^{\mathrm{relax}}$ accounts for the space lag of the ionic atmosphere compared to the central ion, and is not so easy to calculate in the system. When an ion moves forward, its ionic atmosphere takes a short time to follow, of the order of the Debye time τ_{D}. So, the ionic atmosphere has a time delay of the order of the Debye time, and has a space lag of the order of the Debye time times the velocity of the central ion. Due to this space lag, an electrostatic force draws back the central ion. Both effects were found and calculated by Onsager[28]. Newton's equation for the motion of an ion becomes, writing the hydrodynamic coupling as a force

$$m_i^* \frac{\mathrm{d}\boldsymbol{v_i}}{\mathrm{dt}} = \boldsymbol{F}_i^{\mathrm{el}} + \boldsymbol{F}_i^{\mathrm{friction}} + \boldsymbol{F}_i^{\mathrm{hyd}} + \boldsymbol{F}_i^{\mathrm{relax}} \tag{9}$$

or, writing also the inertia part as a force

$$0 = \boldsymbol{F}_i^{\mathrm{el}} + \boldsymbol{F}_i^{\mathrm{friction}} + \boldsymbol{F}_i^{\mathrm{hyd}} + \boldsymbol{F}_i^{\mathrm{relax}} + \boldsymbol{F}_i^{\mathrm{inertia+pressure}} \tag{10}$$

i.e.

$$\boldsymbol{v}_i - \boldsymbol{v}_{\mathrm{s}} = \frac{D_i^\circ}{k_B T}(Q_i \boldsymbol{E} - j\omega m_i^* \boldsymbol{v}_{\mathrm{s}}) + \boldsymbol{F}_i^{\mathrm{hyd}} + \boldsymbol{F}_i^{\mathrm{relax}} \tag{11}$$

As hydrodynamic and electrostatic relaxation forces are corrections dependent on concentration, they are small at low concentration, up to a concentration of 10^{-2} mol L^{-1} for small electrolytes. The Debye theory corrected for the buoyancy is thus reliable up to about 10^{-2} mol L^{-1}, with an IVP independent of the concentration between 5×10^{-4} and 10^{-2} mol L^{-1}.

The corrective forces involve the total correlation function $h_{ij}(r) = g_{ij}(r) - 1$ with $g_{ij}(r)$ the radial distribution function at equilibrium between species i and j. To calculate these quantities, we use integral equations, namely the mean spherical approximation (MSA), which is an approximative solution of the primitive model where ions are modeled as charged hard spheres[30]. Note that Onsager's formulation of these corrections was based on the Debye-Hückel theory, which neglects excluded volume effects. The parameters of the primitive model are the dielectric permittivity of the solvent ε_{r}, the charges of ions Q_i and the minimal distance of approach between ions, i.e. the diameter of ions σ_i. The equations for the hydrodynamic forces can be found in[9] and are summarized in Appendix A (section 7.1) with notations consistent with those used in the present article. Moreover, we improved the precision of the calculation of these contributions by inserting the result of one force in the calculation of the other in a self-consistent way. As already mentioned in the introduction, note that the framework of this analytical theory was already used successfully to account for other transport coefficients in electrolyte and micellar solutions[24–27].

2.3 All relevant input parameters can be determined by independent experiments

The parameters needed to compute the IVP are thus: the relative permittivity of the solvent ε_{r}, the ionic concentrations C_i, the ionic charges Q_i, the self-diffusion coefficients of ions at infinite dilution D_i°, the masses of ions m_i, the partial molar volumes of ions V_i, and the diameters of ions σ_i. Note that the diameters σ_i are only involved in the calculation of the corrective forces.

The relative permittivity of the solvent is that of pure water at 298 K. Charges and masses are of course unambiguously known for ions. Moreover, a considerable amount of data on ions are available in the literature, e.g. Marcus' book[31], where the self-diffusion coefficients at infinite dilution D_i° (or the molar electric conductivity at infinite dilution λ_i°) and the partial molar volumes V_i can be found.

The choice of the ionic radius is not so obvious, because several definitions exist, the most commonly used being the crystallographic radius and the Stokes-Einstein radius. The crystallographic radius or Pauling radius is obtained from X-ray diffraction and measures the cation-anion distance in the solid state. The Stokes-Einstein radius R_{h}, or hydrodynamic radius, is deduced from the diffusion coefficient at infinite dilution ($D_i^\circ = k_B T/(6\pi\eta R_{\mathrm{h}})$). Actually, in the range where the corrective forces are negligible (dilute range, $c < 10^{-2}$ mol L^{-1}), the radii have no influence on the theoretical IVP and the Debye formula is reliable. At high concentration ($c > 10^{-2}$ mol L^{-1}), the corrective forces must be taken into account and are usually strongly influenced by the value of the radii. In the intermediate range, the corrective forces must be taken into account but are only slightly influenced by the value of the radii. As cations and anions are

strongly attracted by each other in the solid state but can be hydrated in water, the crystallographic radius can be assumed to provide an inferior limit for the minimal distance of approach used in MSA. Actually, if the radius is smaller than the Stokes-Einstein value, the hydrodynamic correction to the motion can be larger than the ideal contribution in the concentrated range, an artefact which leads to a negative conductivity. As a consequence, we take in every case for the radius the largest value between the crystallographic radius and the Stokes-Einstein one.

3 Measurement of the IVP and CVP

3.1 Historical background

On the experimental side, some historical elements are also useful to better understand our approach. The first experiments to test the prediction of Debye were performed only 13 years later, in 1946, on colloids[32], and remained qualitative. Several years were then necessary to identify and solve difficulties linked both to the small electrical signal produced by the acoustic excitation and to several "false effects" which raised doubts about the theoretical prediction. Finally two groups ended with laboratory devices performing quantitative measurements on electrolytes[4,33] or colloidal systems of polyelectrolytes or micelles[3]. Only the amplitude of the raw signal (difference of potential IVP or CVP between two electrodes) was measured, not its phase. The quantitative measurements on electrolytes were used by Zana et al to extract partial molar volumes[3].

From 1985 were developed three commercial devices by three different groups, who also proposed a theoretical approach coupled to their devices. All were oriented toward the determination of the zeta potential of colloidal objects, especially in concentrated dispersions. Marlow developed a device working with stationary waves giving a CVP (Pen Kem 7000 by Pen Kem, 1988)[10] no longer available nowadays. In parallel, O'Brien et al developed a device working in the inverse mode, called ElectroSonic Amplitude (ESA): pulses of electric potential at typically 1 MHz are applied to the solution and the acoustic signal produced is detected. The Acoustosizer II by Colloidal Dynamics is a currently available commercial device using this inverse mode, associated with the theoretical treatment developed by O'Brien[34]. Finally, Dukhin et al developed a currently available device (DT1200, Dispersion Technology, 2002) working in the direct mode with acoustic pulses however measuring a current, called colloidal vibration intensity (CVI) and not designed for electrolytes[20]. The signal is treated by the theoretical approaches by Dukhin et al[11]. These two latter devices need a preliminary calibration (with a colloidal system) and give both the amplitude and the phase of the signal. Designed for colloidal systems, they convert the raw signal into a mobility and a sign of the charge of the colloidal species, quantities then converted into zeta potential using models, the details of which remain unknown for the user.

3.2 The new experimental setup

In order to measure the low signals, first here in electrolytes, later on other systems, on small sample volumes and without calibration, we developed a device based on the direct mode, i.e. measuring IVP/CVP. The setup has been developed in partnership with Cordouan Technologies SAS; a patent on this new arrangement is pending[35,36]. Figure 1 provides a diagram which indicates the main elements as well as the notations used in the text.

Three parts are necessary: (i) an acoustic excitation, produced by a transducer and propagated towards the samples cell; (ii) a cell, where 2 electrodes are placed for detection of the signal; (iii) an electronic system for the detection of the voltage induced between these 2 electrodes. The difficulties arise here from the strong interconnections between the three parts, so that only a global approach can result in an optimization of the device. For our purpose, the acoustic frequency chosen is 1 MHz, which corresponds to a wavelength $\lambda = 1.5$ mm in water. The acoustic pressure in the sample is around 70000 Pa, which corresponds to a solvent velocity of 0.045 m s^{-1}. In practice, the real value of pressure is precisely mapped in situ with an hydrophone: the pressure is quasi homogeneous on a disk in the center of the cell, where the electrodes E_1 and E_2 are located. Acoustic pulses of 15 to 25 periods are used in order to separate excitation and detection thanks to a delay line. The wall of the cell first reached by the acoustic wave (W_1) has an acoustic impedance close to that of water, which minimizes losses while the opposite wall of the cell (W_2) is an absorbent material in order to eliminate acoustic reflexions on the wall of the cell which would perturb

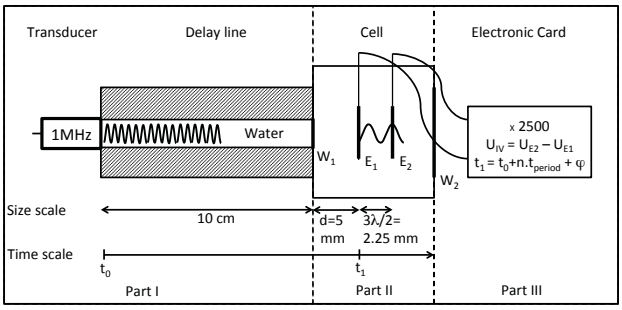

Fig. 1 Diagram showing the main elements of the device, with notations used. Note that scales vary depending on the part for practical reasons.

the signal. The volume of the actual cell is 4 mL and will be optimized in the future to reduce it to 1–2 mL. The potential created in the sample is measured with two electrodes at a distance of $3\lambda/2$, here 2.25 mm. The distance is experimentally measured thanks to a microscope using a x40 lens (accuracy $\pm$ 5 μm). The signal is treated by an electronic card which filters at 1MHz and amplifies by a factor around 2500, precisely determined on a dummy cell before measurements. Averaging is directly made on the oscilloscope and the signal obtained always looks like the example plotted in Figure 2.

From this signal, the amplitude U_{IV} and the phase φ are determined in the area where a quasi stationary state is reached, here between the 10^{th} and the 25^{th} periods of the signal. The amplitude U_{IV} is the average over all these periods. It will be presented hereunder normalized by the pressure as S_{IV} $=U_{IV}/\Delta P$ (see Equation 8). The quality of the signal is here evaluated by comparing the signal to the maximum of the noise determined between two acoustic impulsions. This noise is plotted as error bar on the graphs presented. The reproducibility of the measurements with the device was checked on several electrolytes as well as on $K_4SiW_{12}O_{40}$: it is better than 5%.

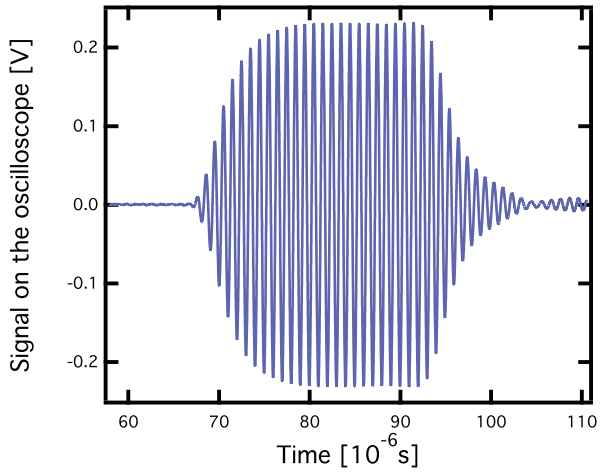

Fig. 2 Example of a real signal measured on the oscilloscope with the conditions given in the text. Sample shown : $K_4SiW_{12}O_{40}$ at 0.003 mol/L.

The phase φ is determined from the delay between the excitation and the signal (t_1-t_0), provided that a definition is chosen. By convention, we decide here that φ=0 when the difference of potential U_{E_2}-U_{E_1} is maximum for a maximum of pressure on electrode 2 (case plotted in Figure 1).

Up to now, the underlying hypothesis is that the speed of sound in the samples v_{sample} is very close to the speed of sound in water v_{water}. This is true here for all systems except for solutions of $BaCl_2$ and $K_4SiW_{12}O_{40}$ at high concentrations. Speeds of sound are taken from literature[37,38] or measured with an Anton Paar DSA 5000 M. When v_{sample} is modified, the acoustic wavelength is modified and the inter-electrode distance does no longer match with the condition $3\lambda/2$. The real amplitude U_{IV}^{real} is then recalculated from U_{IV}^{exp} as U_{IV}^{real} = U_{IV}^{exp} . $1/\cos(2\pi\Delta\lambda/\lambda)$. The phase φ is corrected by taking into account the change of the delay (t_1-t_0) due to the different speed of sound in the cell. The delay becomes t_1-t_0+Δt $=(d+3\lambda/4)(1/v_{water}-1/v_{sample})$ (see notations in Figure 1).

In the experiments presented in the next sections, temperature is 20°C. Note that its influence on S_{IV} is weak because temperature essentially affects viscosity, therefore D_i^o, parameter which appears both in numerator and denominator in equation 5 in such a way that there is compensation.

We underline the fact that our device gives absolute values once the acoustic pressure and the position of the electrodes are known. This is important as it avoids the difficulties associated with calibration. Indeed calibration is easy using the large signals given for example by appropriate large colloids, for which the expected signal is difficult to precisely estimate. On the contrary, calibration could be done with electrolytes, for which the signal can be calculated, however their signals are small. In the following, electrolytes are used as models in order to experimentally check the validity of our new device.

4 Results

4.1 The electrostatic relaxation force has a negligible influence on the IVP for solutions with only two ionic species

The electrostatic relaxation force $\boldsymbol{F}_{\text{relax}}$ is due to the space lag between an ion and its ionic atmosphere, which is due to the velocity differences between ionic species. In an electrolyte solution with only two ionic species, this force is actually negligible in the whole concentration range. We provide quantitative details of this result in appendix B in section 7.2.

As shown before, the high concentration regime is equivalent to low frequency ($\omega\varepsilon_o\varepsilon_r/K \ll 1$), and at low frequency, there is almost no net electric current through the solution (since a net electric current leads to an accumulation of charges over time, which leads to a non-physical divergence of the electric field). In a binary electrolyte, zero net current means that the current due to the anion velocity is the opposite to that due to the cation velocity; therefore, both anions and cations have the same velocity. If both anion and cation have the same velocity, there is no space lag between an ion and its ionic atmosphere, and thus no electric relaxation force. Note that for the ESA and CVI, there is no such zero net current condition, so that there is no cancellation of the electric relaxation term, and no simplification of the equations.

In the low concentration regime, the condition $\omega\varepsilon_o\varepsilon_r/K < 1$

does not hold, so there is no zero net current condition. However, at the frequency used (1 MHz), low concentration means concentration smaller than 5×10^{-4} mol L^{-1}. In this concentration range, it has been known since Onsager that the electrostatic relaxation force is very small, so that it is neglected in what follows.

In conclusion, the calculation of the IVP is easy for a binary electrolyte, with the only corrective force being the electrophoretic one. Finally, three different regimes are observed for the IVP as a function of the concentration: a linear behavior at very low concentration ($< 5 \times 10^{-4}$ mol L^{-1}), then a plateau ($5 \times 10^{-4} - 10^{-2}$ mol L^{-1}), and a final evolution of the IVP at higher concentration due to the electrophoretic force, increasing or decreasing with the concentration depending on the nature of ions (see section 4.4).

4.2 Experimental evidence for the necessity to account for the buoyancy force

As the buoyancy force has not been always taken into account in the literature, its relevance is not obvious for electrolytes. An answer to this question is obtained here with two electrolytes with extreme behaviors depending on the hypothesis. Indeed, the expected signal can be easily calculated without and with this contribution. The best systems to discriminate are therefore electrolytes for which one hypothesis gives no signal while the other one gives a signal.

The first appropriate salt is $Ba(NO_3)_2$. If the buoyancy force is not taken into account, the IVP is almost zero because of the compensation of the products $D_i^\circ m_i^*$ for the cation and the anion (see the data in Table 1). In the opposite case, $|S_{IV}| = 2.4 \times 10^{-10}$ V Pa^{-1} in the concentration range where corrections can be neglected. The second appropriate salt is $Sr(ClO_4)_2$ for which the situation is opposite: the IVP would be $|S_{IV}| = 3.65 \times 10^{-10}$ V Pa^{-1} without buoyancy force and close to zero with this buoyancy force.

Experimentally, for a baryum nitrate solution with concentration 0.01 mol L^{-1}, a signal is clearly observed with our device, with a value $|S_{IV}| = 2.37 \times 10^{-10}$ V Pa^{-1}, close to the expected value. For a strontium perchlorate solution at 0.01 mol L^{-1}, our device shows a small signal around $|S_{IV}| = 1.54 \times 10^{-11}$ V Pa^{-1}, indicating that the IVP is close to zero. Therefore, these two measurements confirm that the buoyancy force has to be taken into account in the theoretical treatment and that the calculations using the partial molar volumes is appropriate.

4.3 Measurements with the new setup are consistent with the theory and previous data

Our setup can now be tested in details on a series of measurements using an electrolyte on a large concentration range, here for $BaCl_2$ between 10^{-4} and 1 mol/L. Values are then compared with the theory presented here and with literature[4] (see Figure 3). Firstly, we check on the whole series that the exact model without buoyancy force is clearly not adapted, as derived in the previous section on extreme situations. Secondly, comparisons between theory and experiment can be split in two regions. At lower concentrations, where Zana has no data, a clear decrease of the signal is observed as predicted by the theory however the values are lower than expected from the theory. In this dilute region, the theory is reliable however measurements are very difficult. The signal is low as well as the conductivity, therefore the impedance of the solution increases and comes closer to the input impedance of the detection system. Also the short cables between the electrodes and the detection interfere. These phenomena are not fully compensated yet on the present system and lead to a systematic bias with an underestimation of the signal in some situations at low concentration. On the contrary, at concentrations larger than 0.001 mol L^{-1}, data are in good agreement with those of Zana and with the theoretical predictions. Note that the setup of Zana did not need calibration. However, contrary to our device, very large volumes (> 100 ml) of sample were needed. Also the frequency was 220 kHz, which would shift the rising part of the theoretical curve on the left compared to our case here with a frequency of 1 MHz. The good agreement between measurements and theory without adjustable parameter and calibration thus enables validating the setup for sufficiently conductive solutions.

Table 1 Data used in the model for the electrolytes presented in water at room temperature: molar mass M_i, diffusion coefficient D_i° at infinite dilution, the relevant parameter $M_i^* D_i^\circ$ where the effective molar mass $M_i^* = M_i - \rho_s V_i$, partial molar volume V_i and diameter σ_i. For all simple ions, D_i° and V_i values are taken from Marcus[31] with his underlying hypothesis that $V_{H^+} = -5.5$ cm^3 mol^{-1}. For $SiW_{12}O_{40}^{4-}$, ranges of values are taken from literature for D_i° and σ_i; we determined V_i (see text for details).

Ion	M_i g mol^{-1}	$10^9 D_i^\circ$ m^2 s^{-1}	V$_i$ cm^3 S.I.	$10^{12} M_i^* D_i^\circ$ mol^{-1}	σ_i nm
H^+	1	9.311	-5.5	60.5	0.190
K^+	39.1	1.957	3.5	69.7	0.276
Cs^+	132.9	2.056	15.8	240.8	0.340
Mg^{2+}	24.3	0.706	-32.2	39.9	0.694
Sr^{2+}	87.6	0.791	-29.2	92.4	0.619
Ba^{2+}	137.3	0.847	-23.5	136.2	0.579
Cl^-	35.45	2.032	23.3	24.7	0.362
NO_3^-	62	1.902	34.5	52.3	0.382
ClO_4^-	99.5	1.792	49.6	89.4	0.472
$SiW_{12}O_{40}^{4-}$	2874.14	0.39-0.56	534	1170.1	0.92-1.3

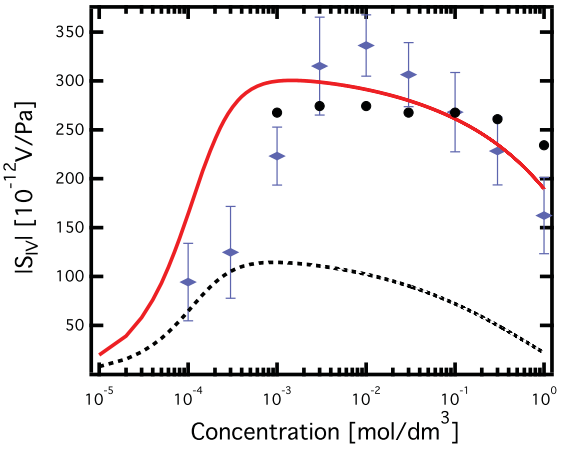

Fig. 3 Comparison of the magnitude of the Ionic Vibration Potentials for $BaCl_2$ in water at 20°C measured with our setup (blue diamonds) and obtained by Zana[4] (black circles). These latter have been renormalized by the acoustic intensity to be comparable to our measurements. The red line is the calculated $|S_{iv}|/P$ with all terms and the black dashed line is the calculated $|S_{iv}|/P$ without the buoyancy term for comparison.

4.4 The evolution of the IVP at high concentration is understood thanks to the theory

Let us now focus on the high concentration part of the IVP as a function of concentration (i.e. the low frequency ($\omega\varepsilon_o\varepsilon_r/K \ll 1$)). In this concentration range, the IVP was predicted constant by Debye. In this regime, corrective forces are needed in the theory, and, as stated before, the only corrective force involved is the hydrodynamic one. It is null at low concentration, since ions are far from each other and undergo no hydrodynamic coupling, and is an increasing function of the concentration, since interionic distances decrease as concentration increases. To understand the effect of the hydrodynamic force and in particular to predict if the IVP is an increasing or a decreasing function of the concentration, we first use a simplified version of MSA in which both anions and cations have the same size, and neglect the imaginary part of the conductivity. We get the following equation, reminiscent of equation 8:

$$S_{\mathrm{IV}} = \frac{1}{\rho_s}\frac{m_+^*(D_+^\circ - H_+) - m_-^*(D_-^\circ - H_-)}{Q_+(D_+^\circ - H_+) - Q_-(D_-^\circ - H_-)} \qquad (12)$$

where $H_\pm$ accounts for the contribution of the hydrodynamic force, so it has a zero value at high dilution and is an increasing function of the concentration; in this simplified version with the same size for both ions, H_+=H_-=H. The sign of the slope at high concentration is given by W with:

$$W = \frac{1}{S_{\mathrm{IV}}}\left(\frac{\mathrm{d}S_{\mathrm{IV}}}{\mathrm{d}H}\right)_{H=0} = \frac{(m_-^*Q_+ - m_+^*Q_-)(D_+^\circ - D_-^\circ)}{(Q_+D_+^\circ - Q_-D_-^\circ)(m_+^*D_+^\circ - m_-^*D_-^\circ)} \qquad (13)$$

If both ions have positive effective masses, which is the case for most inorganic salts, W has the same sign than the following simplified expression:

$$\mathrm{sign}(W) = \mathrm{sign}\left(\frac{D_+^\circ - D_-^\circ}{m_+^*D_+^\circ - m_-^*D_-^\circ}\right) \qquad (14)$$

Three situations can occur:

- Case 1: if $D_+^\circ = D_-^\circ$ then $W = 0$
- Case 2: if the anion has a high diffusivity D_-° and a low effective mass m_-^*, then the numerator is negative and the denominator positive, so W is negative and the IVP decreases as the concentration increases.
- Case 3: if the anion has a high diffusivity D_-° and a high effective mass m_-^*, then both the above numerator and the denominator are negative, so W is positive and the IVP increases as the concentration increases. The same occurs when both anion and cation have the same effective mass.

Thus the simplified formula predicts three possible evolutions at high concentrations. Note that, if the hydrodynamic coupling was taken into account only on the electrostatic force, we would obtain S_{IV}=$\frac{1}{\rho_s}\frac{m_+^*D_+^\circ - m_-^*D_-^\circ}{Q_+(D_+^\circ - H) - Q_-(D_-^\circ - H)}$ so that S_{IV} would only increase when the concentration increases. The decrease of S_{IV} at high concentration can thus be explained only if hydrodynamic coupling induced by inertia is taken into account.

As it can be seen in Figures 3 and 4, the three different behaviors at high concentration are actually observed experimentally and reproduced by the full theory. Cesium chloride, CsCl, corresponds to case 1 (Figure 4) , $BaCl_2$ corresponds to case 2 (Figure 3), obtained for most chloride salts, and $Mg(ClO_4)_2$ corresponds to case 3 (Figure 4). Note however that the values of the IVPs strongly differ depending on the salt: at 0.01 mol L^{-1}, $|S_{IV}|(CsCl)=5.48\times10^{-10}$ V Pa^{-1}, $|S_{IV}|(BaCl_2)=2.88\times10^{-10}$ V Pa^{-1} and $|S_{IV}|(Mg(ClO_4)_2)=1.68\times10^{-10}$ V Pa^{-1}. The agreement between experiment and theory is very good for CsCl even at low concentration, and rather good for $BaCl_2$ as already discussed. For $MgClO_4$, $S_{IV}^{exp} < S_{IV}^{calc}$, which may be the consequence of the low signal. However a clear increase of the potential is observed at high concentration, which was never reported in literature.

Note that when the signal predicted without corrective forces is zero, a non zero signal can be created at large concentrations due to the corrective forces. This is illustrated by

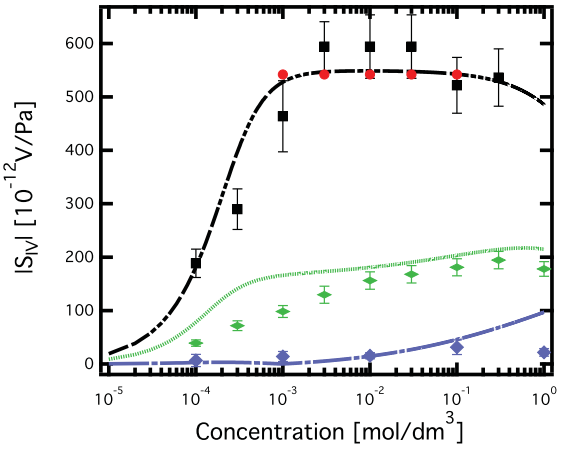

Fig. 4 Experimental magnitude of the Ionic Vibration Potentials for CsCl (■), $Mg(ClO_4)_2$ (green horizontal diamonds) and $Sr(ClO_4)_2$ (blue ♦) at 20°C. The data of Zana for CsCl are plotted (red •). The theoretical curves are plotted as lines for each salt (same color as symbols).

the aqueous solutions of the salt $Sr(ClO_4)_2$ (see Figure 4), for which the maximal amplitude of the measured signal is $|S_{IV}|$=3.15×10^{-11} V Pa^{-1}, i.e; much lower than the previous salts. In such a case, the calculated curve becomes very sensitive to the introduced parameters.

4.5 A first step towards colloids: solutions of small nanoparticles

A first step towards larger objects like colloids can be done using macroions, which can be considered as small nanoparticles. Polyoxometallates as $K_4SiW_{12}O_{40}$ are good models. The anion is monodisperse and roughly spherical with a negative charge of $z = -4$ and a diameter σ close to 1 nm. It corresponds to a rather large density of charge of 1.3 charge per nm^2 similar to those found for nanoparticles.

In practice, only the acidic salt $H_4SiW_{12}O_{40}$ can be bought (Aldrich). We first determined the hydration number $n = 23.6$ from the average of several weight determinations after dehydration at 110°C. The acidic solutions are then neutralized by KOH up to pH< 4. Indeed, for larger pH, the silicotungstate is hydrolyzed so that it is no longer the same system. Therefore the pure system $K_4SiW_{12}O_{40}$ cannot be prepared for very low concentrations as an H^+ concentration larger than 1×10^{-4} mol L^{-1} is present. It means that for [$K_4SiW_{12}O_{40}$]< 0.001 mol L^{-1}, [H^+] is no longer negligible. Here, the electroacoustic signal was measured in the range 0.0001–0.1 mol L^{-1} (see Figure 5), therefore the results for the most dilute samples should be considered with caution. Note also that [$K_4SiW_{12}O_{40}$]=0.01 mol L^{-1} at the maximum of $|S_{IV}|$ corresponds to a weight fraction of 3.2% therefore to a volume fraction around 0.6%.

For the theoretical calculation, the partial molar volume is determined from density measurements at 298 K with an accuracy of 10^{-6} on an Anton Paar DSA 5000 M on a series of solutions prepared by weight with an accuracy of 10^{-5} on the weight in degassed water. Densities were measured on a large range of molalities from 0.00016 to 0.18 mol/kg (0.00015 to 0.165 mol L^{-1}) for $H_4SiW_{12}O_{40}$. From the experimental densities, which are in perfect agreement with those of Sadeghi[38] in the range he reported, we followed the method used in[39] to derive the molar volume. We obtained 512 cm^3 mol^{-1} for the volume of $H_4SiW_{12}O_{40}$ on the whole range of concentration. The value for the anion $SiW_{12}O_{40}^{4-}$ given in Table 1 is then determined using the same assumptions $V_{H^+} = -5.5$ cm^3 mol^{-1} as the one used for the other values of the table. The diameter of $SiW_{12}O_{40}^{4-}$ depends on the method to estimate it. The diameter corresponding to the distance between the silicon central atom and the external oxygen atom is 1.05 nm[40]; the diameter calculated from the volume determined at infinite dilution here is 1.19 nm; the diameter estimated from the radial distribution functions calculated by simulations gives 1.2-1.3 nm[41]. The diffusion coefficient has been determined in literature by several authors leading to values between 0.39 × 10^{-9} m^{2}s^{-1} and 0.56 × 10^{-9} m^{2}s^{-1} [40,42–45].

As a consequence, the values of these two parameters, size and diffusion coefficient, are fitted so that the theoretical curve accounts at best for experimental results. Note that the influence of the diameter is weak and only slightly modifies CVP values at concentrations larger than 0.01 mol/L. On the contrary, the diffusion coefficient influences the whole curve, CVP increasing typically by 40% on the range of coefficients taken from literature. As shown in Figure 5, the data are fully compatible with theoretical curves with D°= 0.56 × 10^{-9} m^{2}s^{-1} and diameter σ = 1.3 nm.

From such measurements, within the hypothesis that the signal is dominated by the contribution of one colloidal specie, a value of the mobility μ of this colloidal specie can be estimated. From the previous formalism (Equation 7), it can be demonstrated that the signal can be rewritten as:

$$U_{IV} = \frac{\Delta P}{K^*}\phi_{wt}\mu\frac{\rho - \rho_{suspension}}{\rho} \qquad (15)$$

where ϕ_{wt} is the weight fraction of the colloid, ρ is a density calculated as the molar mass divided by the partial molar volume for the colloid and $\rho_{suspension}$ is the density of the suspension. This is therefore not valid for electrolytes. Here the nanocolloid is $SiW_{12}O_{40}^{4-}$, which dominates the signal, and ρ=5.39 g/cm^3. We obtain here μ = 6.9 ± 0.05 10^{-8} m^2 V^{-1} s^{-1} at 0.01 mol/L. This value is lower than the mobility at infinite dilution μ° = 8.7 10^{-8} m^2 V^{-1} s^{-1}, obtained using the value D°= 0.56 10^{-9} m^{2}s^{-1}, as expected due to the interac-

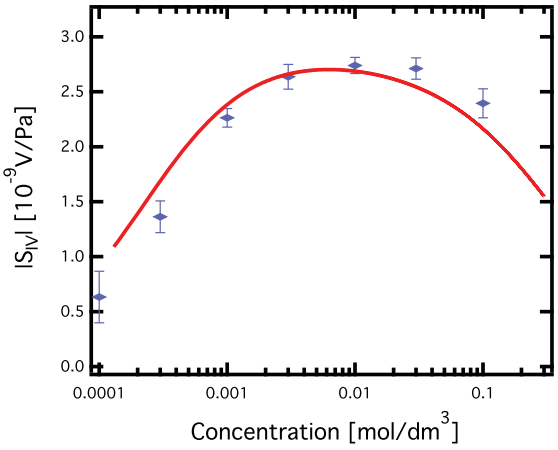

Fig. 5 Magnitude of the Ionic Vibration Potentials for $K_4SiW_{12}O_{40}$: experimental data at 20°C with our new setup (blue ♦) and the theoretical curve (red line). Parameters: $[H^+]$=0.005 M, $D°$=0.56 10^{-9} m^2s^{-1}, diameter σ=1.3 nm. See text for details.

tions between ions in such a concentrated suspension. For systems made of larger particles, μ can be obtained in the same way and transformed into a ζ potential, values which could be compared with other techniques as laser Doppler velocimetry. Unfortunately, the tungstosilicate ion is too small for such scattering based measurements.

4.6 The phase gives the sign of the charge of the heavier species

As explained in section 3.2, the phase φ can be measured. In the case of electrolytes, its value at high concentration is linked to the sign of the heavier species. Following our convention, the phase φ at high concentration is expected to be $\varphi = 0$ for CsCl and $\varphi = 180°$ for $K_4SiW_{12}O_{40}$. This is checked once with a hydrophone placed in the plane of the electrode E_2 while measuring S_{IV}(CsCl). Figures 6 show that the heavier species is indeed the cation for CsCl and $BaCl_2$ and the anion in $MgClO_4$ and $K_4SiW_{12}O_{40}$.

If the concentration decreases, the phase is modified due to the imaginary part of the conductivity $K^*(\omega)$, which cannot be neglected. In this range, the response of the system is delayed, therefore the phase is negative with a maximal shift of 90°. This is the trend observed for all systems, however there is only a qualitative agreement with theory. The results for $Mg(ClO_4)_2$ show the difficulty for the phase determination with a very low signal. Indeed, deviations can arise from the non linearity of capacitive phenomena versus the amplitude of the signal. Independently, the phase can be shifted by a slight asymmetry between the capacitive compensations of the connections between the electrodes and the electronic device. These weaknesses will be corrected in the forthcoming electronic circuit.

These results on the phase nevertheless validate its measurement at large enough concentrations with the present system. This parameter is important for the determination of the sign of the charge of the particles in an unknown system of particles.

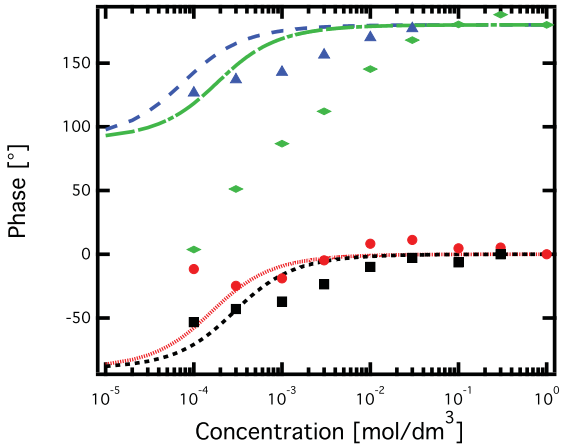

Fig. 6 Phases of the Ionic Vibration Potentials for CsCl (black ■ and dotted black line), $BaCl_2$ (red dots and plain red line), $K_4SiW_{12}O_{40}$ (blue ▲ and dashed blue line) and $Mg(ClO_4)_2$ (green ♦ and dotted-dashed green line): theoretical predictions (lines) and values (symbols) obtained with our new device at 20°C.

5 Conclusion

In the present work, we developed a theory for the ion vibration potential IVP, quite close to the reliable theory of the electrical conductivity of the literature, and built in parallel a device for measuring these small electroacoustic signals on small volumes close to 4 mL. Measurements of the IVP on several electrolyte solutions were done, which validate the ability to measure their small signal in a reproducible and reliable way with our setup. With our dual approach, we clearly explain and validate the different contributions to the IVP, in particular the necessity to consider the buoyancy force, and to properly implement the corrective forces at large concentrations. The evolution of the signal in several typical cases is explained by the theory without adjustable parameter.

The measurement on a system of small nanoparticles (tungstosilicate ions) opens the way towards larger colloidal objects, the CVP signal of which may dominate or may be small and/or mixed with the one of the surrounding electrolyte. In such systems, a mobility can be extracted from CVP, and later converted into a ζ potential. This mobility can

be compared to results obtained by other techniques measuring this mobility as Laser Doppler Velocimetry. We already began measurements of the CVP for different kinds of larger nanoparticles solutions, which will be reported in forthcoming publications.

6 Acknowledgements

The authors would like to thank Cordouan Technologies SAS (www.cordouan-tech.com) for its financial support and participation to the development of the new experimental setup for electroacoustic measurement presented here. Partial financial support of the Agence Nationale de la Recherche in the frame of the project Celadyct (ANR-12-BS08-0017-01) is also gratefully acknowledged. The authors also thank Pierre Turq for helpful discussions and Juliette Sirieix-Plénet for help with the measurements of partial molar volume.

7 Appendix

7.1 A: Hydrodynamic corrective force in the framework of the MSA-transport theory

The hydrodynamic corrective force exerted on ion i is actually proportional to a velocity increment $\delta_{\text{hyd}}\boldsymbol{v_i}$, which is due to the hydrodynamic coupling between the ion i and its ionic atmosphere[9,26,27]:

$$\boldsymbol{F_i^{\text{hyd}}} = \frac{k_B T}{D_i^0}\delta_{\text{hyd}}\boldsymbol{v_i} \tag{16}$$

with

$$\delta_{\text{hyd}}\boldsymbol{v_i} = \sum_j \Omega_{ij}\boldsymbol{F_j} \tag{17}$$

where Ω_{ij} is the coupling between i and j and $\boldsymbol{F_j}$ the force exerted on ion j. $\boldsymbol{F_j}$ is the sum of the hydrodynamic force, the electrostatic relaxation force, the inertia and the buoyancy force. The coupling is related to the total pair correlation function by :

$$\Omega_{ij} = \frac{2}{3\eta}C_j\int_0^\infty r h_{ij}(r)\mathrm{d}r \tag{18}$$

with η the viscosity, C_j the number concentration and h_{ij} the total pair correlation function, which is related to the MSA screening parameter Γ by:

$$\Omega_{ij} = -\frac{1}{3\pi\eta}\frac{Q_iQ_jC_j}{(1+\Gamma\sigma_i)(1+\Gamma\sigma_j)\left(4\varepsilon_0\varepsilon_r k_BT\Gamma + \sum_k C_kQ_k^2\frac{\sigma_k}{(1+\Gamma\sigma_k)^2}\right)} \tag{19}$$

Γ is given by the implicit equation:

$$4\varepsilon_0\varepsilon_r k_BT\Gamma^2 = \sum_i C_i\left(\frac{Q_i}{1+\Gamma\sigma_i}\right)^2 \tag{20}$$

7.2 B: Electrostatic relaxation force

Our aim is here to provide order of magnitudes and an estimation of the phenomena. According to Onsager[28], the electrostatic relaxation is the product of the velocity difference between an ion and its ionic atmosphere by the time delay of this atmosphere and by the electric field gradient at its center. Since the ionic atmosphere around a given ion contains an excess of ions of opposite sign, the velocity difference between the ion ans its ionic atmosphere is roughly equal to the difference between the velocity of cations and anions in a binary electrolyte.

The velocity difference between the cation and the anion is related to the total electric current $\boldsymbol{I}_{tot}$ (assumed to be zero in the main text):

$$\begin{aligned}\boldsymbol{I}_{tot} &= \boldsymbol{I}_+ + \boldsymbol{I}_- \\ &= C_+Q_+\boldsymbol{v}_+ + C_-Q_-\boldsymbol{v}_- \\ &= CQ(\boldsymbol{v}_+ - \boldsymbol{v}_-)\end{aligned} \tag{21}$$

so that

$$(\boldsymbol{v}_+ - \boldsymbol{v}_-) = \frac{\boldsymbol{I}_{tot}}{CQ} \tag{22}$$

Due to the Maxwell Gauss and continuity equations:

$$\boldsymbol{I}_{tot} = j\omega\varepsilon_0\varepsilon_r\boldsymbol{E} \tag{23}$$

so that

$$(\boldsymbol{v}_+ - \boldsymbol{v}_-) = \frac{j\omega\varepsilon_0\varepsilon_r\boldsymbol{E}}{CQ} \tag{24}$$

The time delay of the ionic atmosphere is the Debye time τ_D, with λ_D the Debye length:

$$\tau_D = \frac{\lambda_D^2}{D} \tag{25}$$

$$\lambda_D = \sqrt{\frac{\varepsilon_0\varepsilon_r kT}{C_+Q_+^2 + C_-Q_-^2}} \tag{26}$$

The electric field gradient at the centre of the ionic atmosphere is the local potential divided by the square of the characteristic length, i.e. the Debye length:

$$\nabla E_{center} = \frac{Q}{4\pi\varepsilon_0\varepsilon_r\lambda_D^3} \tag{27}$$

The product of the three terms yields thus the electrostatic field due to the relaxation effect:

$$\boldsymbol{E}^{rel} = \frac{j\omega\varepsilon_0\varepsilon_r\boldsymbol{E}}{CQ}\times\frac{\lambda_D^2}{D}\times\frac{Q}{4\pi\varepsilon_0\varepsilon_r\lambda_D^3} = \frac{j\omega\boldsymbol{E}}{4\pi CD\lambda_D} \tag{28}$$

Above 5.10^{-4} mol/L, the electric field E does not depend on the concentration. Only λ_D and C are concentration dependent and their product scales as $C^{1/2}$. Therefore the electrostatic

field due to relaxation $\boldsymbol{E}^{rel}$ decreases with concentration as $C^{-1/2}$. Under 5.10^{-4} mol/L, the electric field E is linear with C, so that the electrostatic relaxation $\boldsymbol{E}^{rel}$ increases as $C^{1/2}$. The maximum of the electrostatic relaxation is thus reached at 5.10^{-4} mol/L and its value is low, therefore its value remains low on the whole concentration range.

References

1 A. V. Delgado, F. González-Caballero, R. J. Hunter, L. K. Koopal and J. Lyklema, *Pure Appl. Chem.*, 2005, **77**, 1753–1805.
2 P. Debye, *J. Chem. Phys.*, 1933, **1**, 13–17.
3 R. Zana and E. Yeager, *Modern Aspects of Electrochemistry*, Plenum, New York, 1982, vol. 14, ch. 1, pp. 3–60.
4 R. Zana and E. Yeager, *J. Phys. Chem.*, 1967, **71**, 521.
5 S. Oka, *Proc. Physico-Mathematical Soc. Japan. 3rd Ser.*, 1933, **15**, 413–419.
6 J. J. Hermans, *Philos. Mag. Ser. 7*, 1938, **25**, 426–438.
7 J. Bugosh, E. Yeager and F. Hovorka, *J. Chem. Phys.*, 1947, **15**, 592–597.
8 S. Durand Vidal, *PhD thesis*, UPMC, Paris, 1995.
9 S. Durand-Vidal, J.-P. Simonin, P. Turq and O. Bernard, *J. Phys. Chem.*, 1995, **99**, 6733–6738.
10 B. J. Marlow, D. Fairhurst and H. P. Pendse, *Langmuir*, 1988, **4**, 611.
11 A. S. Dukhin and P. J. Goetz, *P. J. Goetz*, Elsevier, Amsterdam, 2002.
12 H. Ohshima, *Theory of Colloid and Interfacial Electric Phenomena*, Academic Press, Amsterdam, 2006.
13 R. W. O'Brien, *J. Fluid Mech.*, 1988, **190**, 71–86.
14 C. Tondre and R. Zana, *J. Phys. Chem.*, 1972, **76**, 3451–3459.
15 J. Khan, M. Wang, H. Schlaberg and P. Guan, *Chem. Phys.*, 2013, **425**, 14–18.
16 A. C. Beveridge, S. Wang and G. J. Diebold, *Appl. Phys. Lett.*, 2004, **85**, 5466–5468.
17 S. Wang, A. C. Beveridge, S. Li, G. J. Diebold and C. K. Nguyen, *Appl. Phys. Lett.*, 2006, **89**, 243902.
18 M. Kosmulski and J. B. Rosenholm, *Adv. Colloid Interface Sci.*, 2004, **112**, 93–107.
19 M. Kosmulski, *Colloids Surfaces A Physicochem. Eng. Asp.*, 2014, **460**, 104–107.
20 A. Dukhin and S. Parlia, *Colloids and Surfaces B: Biointerfaces*, 2014, **121**, 257–263.
21 R. A. Robinson and A. H. Stokes, *Electrolyte Solutions*, Dover Publications, Mineola,New York, 2nd edn, 2002.
22 J. H. Masliyah and S. Bhattacharjee, *Electrokinetic and Colloid Transport Phenomena*, John Wiley & Sons, Inc., Hoboken, NJ, USA, 2006.
23 J. Lyklema, *Fundamentals of Interface and Colloid Science*, Academic Press, San Diego, 1995, vol. 2.
24 O. Bernard, W. Kunz, P. Turq and L. Blum, *J. Phys. Chem.*, 1992, **96**, 3833.
25 S. Durand-Vidal, M. Jardat, V. Dahirel, O. Bernard, K. Perrigaud and P. Turq, *J. Phys. Chem. B*, 2006, **110**, 15542–15547.
26 O. Bernard, W. Kunz, P. Turq and L. Blum, *J. Phys. Chem.*, 1992, **96**, 398.
27 J.-F. Dufrêche, O. Bernard, S. Durand-Vidal and P. Turq, *J. Phys. Chem. B*, 2005, **109**, 9873–9884.
28 L. Onsager and R. M. Fuoss, *J. Phys. Chem.*, 1932, **36**, 2689–2778.
29 S. Gourdin, *et al, forthcoming publication*.
30 L. Blum, in *Theoretical Chemistry: Advances and Perspectives*, ed. H. Eyring and D. Henderson, Academic Press, New York, 1980, vol. 5, pp. 1–66.
31 Y. Marcus, *Ion properties*, Marcel Dekker, New York, 1997.
32 A. J. Rutgers, *Nature*, 1946, **157**, 74–76.
33 R. Millner and H.-D. Müller, *Ann. Phys.*, 1966, **17**, 160–165.
34 R. J. Hunter, *Colloids Surfaces A Physicochem. Eng. Asp.*, 1998, **141**, 37–66.
35 R. Pusset, *PhD thesis*, Université Pierre et Marie Curie, 2013.
36 S. C. Technologies, French patent N° 1361077, 2013.
37 F. J. Millero, G. K. Ward and P. V. Chetirkin, *J. Acoust. Soc. am.*, 1977, **61**, 1492–1498.
38 R. Sadeghi, R. Khoshnavazi, H. Parhizgar and L. Bahrami, *Fluid Phase Equilib.*, 2009, **277**, 87–95.
39 L. Gaillon, J. Sirieix-Plenet and P. Letellier, *J. Solution Chem.*, 2004, **33**, 1333–1347.
40 T. Olynyk, M. Jardat, D. Krulic and P. Turq, *J. Phys. Chem. B*, 2001, **105**, 7394–7398.
41 F. L. Leroy, P. Miro, J. M. Poblet, C. Bo and J. B. Avalos, *J. Phys. Chem. B*, 2015, **to appear**, year.
42 L.C.W.Baker and M.T.Pope, *J. Am. Chem. Soc*, 1960, **82**, 4176–4179.
43 A. Baticle, F. Perdu and P. Vennereau, *C. R. Acad. Sci. Paris, Série C.*, 1967, **264**, 365–368.
44 R. O'Brien, D. Cannon and W. Rowlands, *J. Colloid Interface Science*, 1995, **173**, 406–418.
45 A. Horky, N. Kherani and G. Xu, *J. Electrochem. Soc.*, 2003, **150**, A1219.